

FOURIER SPECTRAL SIMULATIONS FOR WAKE FIELDS IN CONDUCTING CAVITIES *

Misun Min^{†1}, Yong-Ho Chin², Paul F. Fischer¹, Yong-Chul Chae³, Kwang-Je Kim³

¹MCS, ANL, Argonne, IL, 60439 USA, ³APS, ANL, Argonne, IL, 60439 USA

²KEK High Energy Accelerator Research Organization, Ibaraki, 305-0801 Japan

Abstract

We investigate the Fourier spectral time-domain simulations applied to the wake field calculations in two-dimensional cylindrical structures. The scheme involves second-order explicit leap-frogging in time and the Fourier spectral approximation in space, which is obtained from simply replacing the spatial differentiation operator of the YEE scheme by the Fourier differentiation operator [2, 3, 4, 5] on non-staggered grids.

This is a first step towards investigating high-order computational techniques with Fourier spectral method which is relatively simple to implement and enhancing its performance in comparison to the conventional lower-order method.

FORMULATIONS

We study beam dynamics in two-dimensional conducting cavity structures defining the governing equations and the numerical scheme as follows.

Maxwell's Equations

$$\mu \frac{\partial H}{\partial t} = -\nabla \times E, \quad \epsilon \frac{\partial E}{\partial t} = \nabla \times H - J \quad (1)$$

$$\nabla \cdot E = \frac{\rho}{\epsilon}, \quad \nabla \cdot H = 0 \quad (2)$$

where the current source J is defined for an on-axis Gaussian beam moving in x direction

$$J = ce_x \rho(y) \rho(x - ct), \quad \rho(x) = \frac{1}{\sigma_x \sqrt{2\pi}} e^{-\frac{x^2}{2\sigma_x^2}} \quad (3)$$

Numerical Scheme

Let us define the computational domain on $[-L_x, L_x] \times [-L_y, L_y]$ and the grid points as

$$x_i = -L_x + \frac{L_x i}{N_x} (i = 0, \dots, 2N_x - 1) \quad (4)$$

$$y_j = -L_y + \frac{L_y j}{N_y} (j = 0, \dots, 2N_y - 1) \quad (5)$$

We approximate solutions to the Maxwell's equations based on Fourier interpolation polynomials [3, 4] by defining the approximate solution as

$$\bar{E}_{l,k} = \sum_{i=0}^{2N_x-1} \sum_{j=0}^{2N_y-1} E_{i,j} L(x_i) L(y_j) \quad (6)$$

where

$$L(x) = \frac{1}{N_x} \sin \left[N_x \frac{x - x_i}{2} \right] \cot \left[\frac{x - x_i}{2} \right] \quad (7)$$

Then, the Fourier differentiation matrix is given as

$$(\bar{D}_x)_{l,i} = \frac{d}{dx} L_i(x)|_{x_l} = \frac{(-1)^{i+l}}{2} \cot \left[\frac{(i-l)\pi}{2N_x} \right] \quad (8)$$

for $i \neq l$ and $(\bar{D}_x)_{l,i} = 0$ for $i = l$. In a similar manner, \bar{D}_y can be defined. Using tensor product to define the two-dimensional spatial derivatives $D_x = I \otimes \bar{D}_x$ and $D_y = \bar{D}_y \otimes I$ where I represents the identity matrix and representing $\bar{E}_x^n = [(E_x)_{00}, (E_x)_{10}, \dots, (E_x)_{ij}, \dots, (E_x)_{N_x-1, N_y-1}]^T$, our scheme at the time level $t^n = n\Delta t$ is

$$\epsilon \frac{\bar{E}_x^{n+\frac{1}{2}} - \bar{E}_x^{n-\frac{1}{2}}}{\Delta t} = D_y \bar{H}_z^n - \bar{J}_x^n \quad (9)$$

$$\epsilon \frac{\bar{E}_y^{n+\frac{1}{2}} - \bar{E}_y^{n-\frac{1}{2}}}{\Delta t} = -D_x \bar{H}_z^n \quad (10)$$

$$\mu \frac{\bar{H}_z^{n+1} - \bar{H}_z^n}{\Delta t} = D_y \bar{E}_x^{n+\frac{1}{2}} - D_x \bar{E}_y^{n+\frac{1}{2}} \quad (11)$$

Initial Conditions

To describe the electromagnetic fields at the presence of the Gaussian beam for the initial time step, we first solve the Poisson equation in one dimension at the cross section of the initial beam position

$$\nabla^2 \Phi^{1D}(y) = -\frac{\rho^{1D}(y)}{\epsilon} \quad (12)$$

and get the one-dimensional electric field at the cross section

$$E^{1D} = -\nabla \Phi^{1D}(y) \quad (13)$$

Then, the initial electric field E in two dimensions is assigned along the x -direction using the one-dimensional electric field E^{1D} scaled by the initial Gaussian distribution $\rho(x)$ as

$$E(y, x) = E^{1D}(y) * \rho(x) \quad (14)$$

* Work supported by the U.S. Dept. of Energy under Contract DE-AC02-06CH11357.

[†] mmin@mcs.anl.gov

Boundary Conditions

We apply the uniaxial perfectly matched layer (UPML) boundary condition in x -direction and perfectly electric conducting (PEC) boundary condition in y -direction.

UPML formulations are defined in 3D as follows:

$$\frac{\partial H_z}{\partial y} - \frac{\partial H_y}{\partial z} = \frac{\partial D_x}{\partial t} + \frac{1}{\epsilon} \sigma_y D_x \quad (15)$$

$$\frac{\partial H_x}{\partial z} - \frac{\partial H_z}{\partial x} = \frac{\partial D_y}{\partial t} + \frac{1}{\epsilon} \sigma_z D_y \quad (16)$$

$$\frac{\partial H_y}{\partial x} - \frac{\partial H_x}{\partial y} = \frac{\partial D_z}{\partial t} + \frac{1}{\epsilon} \sigma_x D_z \quad (17)$$

where $\sigma_x = -(x/d)^m(m+1)\ln(R)/2\eta d$, denoting d , x , m , R , and η for PML size, the PML depth, polynomial grading, reflection error, and impedance, respectively. Within UPML, the components of E are updated by

$$\epsilon \left[\frac{\partial E_x}{\partial t} + \frac{\sigma_z}{\epsilon} E_x \right] = \frac{\partial D_x}{\partial t} + \frac{\sigma_x}{\epsilon} D_x \quad (18)$$

$$\epsilon \left[\frac{\partial E_y}{\partial t} + \frac{\sigma_x}{\epsilon} E_y \right] = \frac{\partial D_y}{\partial t} + \frac{\sigma_y}{\epsilon} D_y \quad (19)$$

$$\epsilon \left[\frac{\partial E_z}{\partial t} + \frac{\sigma_y}{\epsilon} E_z \right] = \frac{\partial D_z}{\partial t} + \frac{\sigma_z}{\epsilon} D_z \quad (20)$$

A similar formula is defined for the components of H to update in UPML. In our simulations we apply UPML only in x -direction by choosing $\sigma_y = \sigma_z = 0$.

PEC boundary conditions are assigned at the boundaries in y -direction by setting the values for the E and H components as zeros.

COMPUTATIONAL RESULTS

We demonstrate the profiles of wake fields on cylindrical tube and pillbox cavity structures in two dimensions, and discuss the problems we encounter.

Wake fields

Figure 1 shows the electric field profile for y -component on $[-7.5, 7.5] \times [-2, 2]$. at a time step=60 with $\Delta t = \Delta y/10$ and initial beam position at $x = -3.5$. As we expect for the cases with no change in the structures, we observe no significant reflection from the conducting boundary, and the beam is moving with no significant distortion. However we observe visible amount of dissipation around the conducting boundary as the beam moves along the positive direction in x .

We carried out simulations on the pillbox cavity described in Figure 2. Figure 3 shows the electric field profile for y -component on $[-7.5, 7.5] \times [-2, 2]$ for the pillbox configuration in Figure 2. We observe strong oscillations right at the corner of the cavity as soon as the beam enters the cavity and the oscillations remain until the beam passes through out the cavity, which we do not observe from the results obtained in [2, 7].

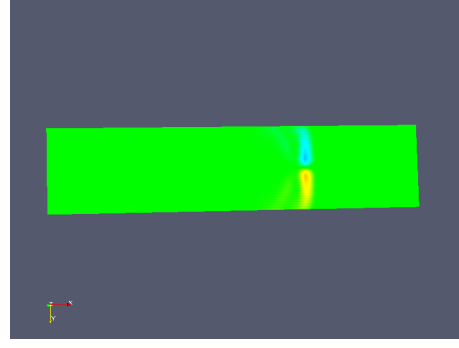


Figure 1: Electric field for y -component on a tube mesh in 2D

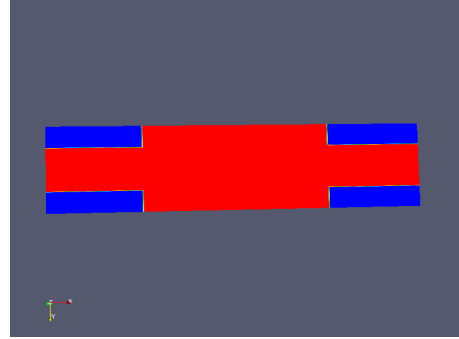


Figure 2: Pillbox cavity structure with PEC region (blue) and vacuum (red) on $[-7.5, 7.5] \times [-2, 2]$; ingoing and outgoing tube radius=1

Discussions

We remain the study on the dissipation and oscillation when using the Fourier spectral scheme we presented in this paper for the wake field calculations with perfect conducting boundary conditions as future works. We have a way to resolve the problems arising with oscillations when using Fourier spectral time domain simulations. One can apply the Gegenbauer or the Padé [5, 6] reconstruction techniques on the Fourier simulation data to remove the unphysical oscillations. Considering wake potential calcu-

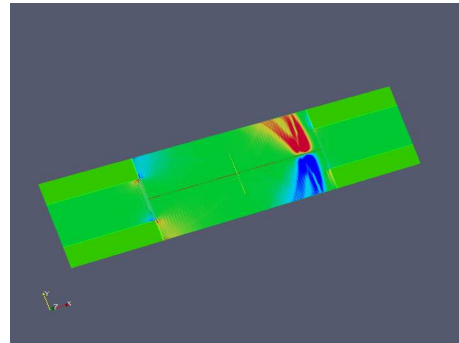


Figure 3: Electric field for y -component on a pillbox mesh in 2D

lation, however, we need to carry out the reconstruction procedures every time step when wake potential calculations are proceeded over the time integrations. This is due to that it is required accurate field values at each time to calculate wake potential not to use the contaminated data from the oscillations. In order to reduce the computational cost for the reconstructions at every step where one has to provide reasonable field values, one can proceed reconstructions locally around the line path where one has to obtain wake potential along. For the pillbox configuration in Figure 2, one can get wake potential along the path $y = 1$ with two-dimensional reconstructions on $[-s, s] \times [1 - \Delta, 1 + \Delta]$ for $s = 5\sigma_x$ and some small Δ .

CONCLUSIONS

We demonstrated Fourier spectral time domain simulations for the wake field calculations on cylindrical tube and pillbox cavity structures. We observe dissipations and unphysical oscillations depending on the structures in the Fourier spectral simulation data. Further study will be carried out in a later paper regarding on how to overcome the difficulties with dissipations and numerical oscillations, and investigate possible enhancement of its performance on the same grid base with 2D wake field calculation code ABCI.

REFERENCES

- [1] Y.C. Chae, "Horizontal Coupling Impedance of the APS Storage Ring", Proc. 2003 PAC (2003), p.3011.
- [2] Y.H. Chin, "User's Guide for ABCI Version 9.4 and Introducing the ABCI Windows Application Package", KEK Report (2005) 2005-06.
- [3] D. Gottlieb, M.Y. Hussaini, and S. Orszag, "Theory and applications of spectral methods", in Spectral methods for partial differential equations, edited by R.G. Voigt, D. Gottlieb, and M.Y. Hussaini, SIAM, Philadelphia (1984).
- [4] D. Gottlieb and C.W. Shu, "On the Gibbs phenomenon and its resolution", SIAM Review, 30, (1997), p.644.
- [5] M.S. Min, T.W. Lee, P.F. Fischer, S.K. Gray, "Fourier spectral simulations and Gegenbauer reconstructions for electromagnetic waves in the presence of a metal nanoparticle", J. of Comp. Phys., 213 (2) (2006), p.730.
- [6] M.S. Min, S.M. Kaber, W.S. Don, "Fourier-Padé Approximations and Filtering for the Spectral Simulations of Incompressible Boussinesq Convection Problem", Math. Comp., 76 (2007), p.1275.
- [7] M.S. Min, P.F. Fischer, and Y.C. Chae, "Spectral element discontinuous Galerkin simulations for wake potential calculations: NEKCEM" these proceedings.